0026-895X/01/6002-235–243$3.00
MOLECULAR PHARMACOLOGY
Copyright © 2001 The American Society for Pharmacology and Experimental Therapeutics
Mol Pharmacol 60:235–243, 2001

Vol. 60, No. 2
668/917210
Printed in U.S.A.

The Noncompetitive Inhibitor Quinacrine Modifies the Desensitization Kinetics of Muscle Acetylcholine Receptors

GUILLERMO SPITZMAUL, JAMES P. DILGER, and CECILIA BOUZAT

Instituto de Investigaciones Bioquímicas, Universidad Nacional del Sur-Consejo Nacional de Investigaciones Científicas y Técnicas, Bahía Blanca, Argentina (G.S.,C.B.); and Department of Anesthesiology, State University of New York Stony Brook, Stony Brook, New York (J.P.D.)

Received October 10, 2000; accepted April 17, 2001

This paper is available online at http://molpharm.aspetjournals.org

ABSTRACT

Quinacrine has been shown to act as a noncompetitive inhibitor of the nicotinic acetylcholine receptor (nAChR). However, its mechanism of action is still a matter of controversy. We analyzed in detail the action of quinacrine at both the single-channel and macroscopic current levels. The main effect of quinacrine is a profound concentration-dependent decrease in both the frequency of opening events and the duration of clusters elicited by high acetylcholine concentrations. Quinacrine also significantly increases (40-fold at 30 μM) the decay rate of macroscopic currents elicited by rapid perfusion of acetylcholine to outside-out patches. This decay is still well-described by a single exponential. Quinacrine has very little effect on the peak amplitude of the response, suggesting that it acts mainly on open channels. The recovery from desensitization after removal of acetylcholine is delayed in the presence of quinacrine. Results from both single-channel and macroscopic current recordings indicate that quinacrine increases the rate of nAChR desensitization and stabilizes the desensitized state. Interestingly, in equilibrium agonist-binding assays, quinacrine does not promote the typical high-affinity desensitized state. Thus, quinacrine seems to induce an intermediate state exhibiting the permeability but not the agonist binding properties of desensitization.

The nicotinic acetylcholine receptor (nAChR) is the paradigm of the neurotransmitter-gated ion channel superfamily. The nAChR is a pentamer of homologous subunits with composition $\alpha_2\beta\gamma\delta$ or $\alpha_2\beta\epsilon\delta$ in embryonic or adult muscle, respectively. The nAChR exists in different functional states: resting, active, and desensitized. The transitions between these states are affected by agonists and competitive antagonists acting at the acetylcholine (ACh) binding sites and by a broad class of noncompetitive inhibitors (NCIs). These inhibitors decrease the probability of channel opening by different general mechanisms: steric blockade of the ion pore, allosteric inhibition of the protein, or enhancement of desensitization.

The acridine derivative quinacrine has been shown to act as an NCI of the nAChR. However, its mechanism of action is still a matter of controversy. Both open-channel blockade and allosteric inhibition of ion flux have been reported (Adams and Feltz, 1980; Valenzuela et al., 1992; Tamamizu et al., 1995; Arias, 1997). In addition, different locations for the quinacrine binding site on the nAChR have been proposed (see review in Arias, 1998). Voltage clamp experiments suggested that quinacrine binding site is located within the ion pore. However, fluorescence quenching and energy transfer studies showed that quinacrine binding sites exist at the lipid-protein interface (Valenzuela et al., 1992; Arias et al., 1993). Arginine209 and Proline211, located at the N-terminal of the αM1 transmembrane domain, have been specifically photolabeled by quinacrine azide (Cox et al., 1985; DiPaola et al., 1990). Measurements of currents evoked by ACh on *Xenopus laevis* oocytes expressing mutant *Torpedo californica* nAChRs showed that mutations at αR209, αP211, and αY213 of *Torpedo* nAChR change the sensitivity to quinacrine (Tamamizu et al., 1995). The M1 domain seems closely associated with both the ion conducting pathway and the lipid bilayer, as revealed by substituted cysteine accessibility and labeling by hydrophobic reagents (Blanton and Cohen, 1994; Akabas and Karlin, 1995). Applying the substituted-cysteine accessibility method to the M1 domain, Akabas and Karlin (1995) have shown that some residues of the N-terminal third of αM1 contribute to the lining of the pore. Residue αP211 is accessible to the hydrophilic reagent only in the absence of ACh.

Here we investigate the mechanistic bases for the noncompetitive action of quinacrine. We describe for the first time the kinetic changes in nAChR at the single channel level and examine the kinetic properties of macroscopic currents. In addition, we compare the effects of quinacrine between adult

This work was supported by National Institutes of Health Grant GM42095 (to J.P.D.), grants from Universidad Nacional del Sur, Agencia Nacional de Promoción Científica y Tecnológica, Ministerio de Salud de la Nacion, and Fogarty International Center Grant 1R03 TW01185–01 (to C.B.).

ABBREVIATIONS: nAChR, nicotinic acetylcholine receptor; ACh, acetylcholine; NCI, noncompetitive inhibitor; HEK, human embryonic kidney; DMEM, Dulbecco's modified Eagle's medium; ECS, extracellular solution; α-BTX, α-bungarotoxin.

and embryonic nAChRs. We conclude that inhibition of nAChR by quinacrine is coincident with an increase in the desensitization rate together with stabilization of a desensitized state, with no significant increase in agonist binding affinity.

Materials and Methods

Expression of nAChR. Mouse cDNAs were subcloned into the cytomegalovirus-based expression vector pRBG4 (Bouzat et al., 1994). HEK293 cells were transfected with α, β, δ, and ϵ cDNA subunits using calcium phosphate precipitation at a subunit ratio of 2:1:1:1, respectively, essentially as described previously (Bouzat et al., 1994, 1998). For transfections, cells at 40 to 50% confluence were incubated for 8 to 12 h at 37°C with the calcium phosphate precipitate containing the cDNAs in DMEM plus 10% fetal bovine serum. Cells were used for patch clamp recordings 1 or 2 days after transfection.

For studying the action of quinacrine on embryonic nAChR, patch clamp recordings were made from BC3H-1 cells. Cells were cultured in DMEM plus 20% fetal bovine serum. After reaching confluence, media was replaced by DMEM plus 10% fetal bovine serum.

Patch-Clamp Recordings. Recordings were obtained in the cell-attached and outside-out patch configurations at 20°C (Hamill et al., 1981). For cell-attached patch recordings, patch pipettes were pulled from 7052 capillary tubes (Garner Glass, Claremont, CA) and coated with Sylgard (Dow Corning, Midland MI). The pipette resistances ranged from 5 to 7 MΩ. The bath and pipette solutions contained 142 mM KCl, 5.4 mM NaCl, 1.8 mM $CaCl_2$, 1.7 mM $MgCl_2$ and 10 mM HEPES, pH 7.4. ACh at final concentrations of 1, 10, or 60 μM and quinacrine at final concentrations of 1, 10, 30, or 60 μM were added to the pipette solution. Channels were typically recorded at a membrane potential of −70 mV. For studying the voltage dependence of the effect of quinacrine on nAChR, channels were also recorded at a membrane potential of −40 and −90 mV and +70 mV. Single-channel currents were recorded using an Axopatch 200 B patch-clamp amplifier (Axon Instruments, Inc., CA) and digitized at 94 kHz with a PCM adapter (VR-10B; InstruTECH, Port Washington, NY). Data were transferred to a computer using the program Acquire (Bruxton Corporation, Seattle, WA) and detected by the half-amplitude threshold criterion using the program TAC 3.0 (Bruxton Corporation) at a final bandwidth of 10 kHz. Open- and closed-time histograms were plotted using a logarithmic abscissa and a square root ordinate and fitted to the sum of exponential functions by maximum likelihood using the program TACFit (Bruxton Corporation). Clusters of openings corresponding to a single channel were identified as a series of closely spaced events preceded and followed by closed intervals greater than a specified duration (ι_{crit}); this duration was taken as the point of intersection of the predominant closed-time component and the succeeding one in the closed-time histogram. For nAChRs activated by 60 μM ACh, the major intermediate component associated to dwell times within clusters typically varied between 0.5 and 1 ms and ι_{crit} between 5 and 8 ms. Cluster duration histograms were constructed and fitted by using the program TACfit setting the burst resolution to the calculated ι_{crit}. Open probability within clusters (P_{open}) was experimentally determined at each ACh concentration by calculating the mean fraction of time the channel is open within a cluster.

For outside-out recordings, patch pipettes were pulled from borosilicate glass, fire polished, and filled with a solution containing 140 mM KCl, 5 mM EGTA, 5 mM $MgCl_2$, and 10 mM HEPES, pH 7.3. Extracellular solution (ECS) contained 150 mM NaCl, 5.6 mM KCl, 1.8 mM $CaCl_2$, 5 mM $MgCl_2$, and 10 mM HEPES, pH 7.3. For outside-out recordings, the patch was excised in this configuration and moved into position at the outflow of a perfusion system. The perfusion system consisted of solution reservoirs, manual switching valves, a solenoid-driven pinch valve, and two tubes (i.d. = 0.3 mm) oriented at 90° inserted into the culture dish (modified from Liu and Dilger, 1991). One tube contained ECS without agonist (normal solution) and the other contained ECS with 300 μM ACh (test solution). The perfusion system allows for a rapid (0.1–1 ms) exchange of the solution bathing the patch. A series of applications (duration 200 ms) of 300 μM ACh were applied to the patch at 5-s intervals. We then recorded the responses of the patch to applications of 300 μM ACh during continuous exposure to different concentrations of quinacrine (1, 3, 6, 10, and 30 μM). After a series of applications of a given quinacrine solution, drug-free solutions were applied to assess loss of channel activity. Macroscopic currents were measured with a patch clamp amplifier (EPC-9; HEKA Electronik, Lambrecht/Pfalz, Germany), filtered at 6.7 kHz, digitized at 20 kHz, and stored on the hard disk. Data analysis was performed off-line with routines written in the IgorPro macro language (WaveMetrics Inc., Lake Oswego, OR). The ensemble mean current was calculated for 10 to 20 individual current traces. Mean currents were fitted by a single exponential function: $I_{(t)} = I_0 \exp(-t/\tau_d) + I_\infty$ where I_0 and I_∞ are the peak and the steady state current values, respectively, and τ_d is the decay time constant that measures the current decay due to desensitization. Current records were aligned with each other at the point at which the current had risen to 50% of its maximum level. Peak currents correspond to the value obtained by extrapolation of the decay current to this point.

To study recovery from desensitization, a double-application protocol was employed. First, a 300-ms application of 300 μM ACh was used to desensitize most of the nAChRs. Then agonist-free solution was perfused for a variable interval ranging from 15 to 435 ms. Finally, a 30-ms agonist application of 300 μM ACh was performed. Agonist-free solution was applied for 5 s in between each pair of applications. To test the action of the drug, quinacrine was present in both control and test solutions. For each pair of agonist applications, we calculated the ratio of the peak of the second current response, I_{02}, and the first current response, I_{01}. The relationship between the ratio of the peak currents and the interval duration (t) was fitted to a single exponential of the form: $I_{02}/I_{01} = 1 - \exp[-t/\tau_r]$, where τ_r is the recovery time constant.

Experimental data are shown as mean ± S.D. Statistical comparisons are done using the Student's t test. A level of $p < 0.05$ is considered significant.

Ligand Binding Measurements. Binding of ACh was measured by competition against the initial rate of [^{125}I]α-bungarotoxin ([^{125}I]α-BTX) binding as described previously (Sine and Taylor, 1979; Sine et al., 1994) and compared with binding in the presence of quinacrine or proadifen. HEK cells expressing adult nAChRs were resuspended in high potassium Ringer's solution in the absence or presence of quinacrine or proadifen and divided into aliquots for ligand binding measurements. Cells were first incubated for 30 min with different concentrations of ACh; [^{125}I]α-BTX was subsequently added to a final concentration of 5 nM, and the cells were incubated for an additional 20 min to allow occupancy of no more than 50% of the binding sites by α-BTX (Sine et al., 1994). The total number of binding sites was determined by incubating cells with 5 nM [^{125}I]α-BTX for 2 h in the absence of ACh. Binding was terminated by the addition of potassium Ringer's solution containing 20 mM carbamylcholine. Nonspecific binding was determined in the presence of 20 mM carbamylcholine. Rates of α-BTX binding in the absence and presence of competing ligand were calculated from binding measured at 20 and 120 min (Fu and Sine, 1996). These rates are related to ligand occupancy by $k_{obs} = k_{max}(1 - Y)$, where k_{obs} is the rate of toxin binding in the presence of a specified concentration of competing ligand, k_{max} is the rate in the absence of competing ligand, and Y is the occupancy function for the competing ligand, given by the Hill equation. Fractional occupancy by ACh was fitted by the Hill equation: 1 − fractional occupancy = $[1/(1 + ([ACh]/K_d)^{nH}]$, where K_d is the apparent dissociation constant and n_H is the Hill coefficient.

Results

Effects of Quinacrine on Single-Channel Currents

Quinacrine Reduces the Frequency of nAChR Opening Events. Adult nAChR channels were recorded 1 and 8 min after seal formation from cell-attached patches using a pipette in which the tip was filled with 1 μM ACh alone and the shaft was filled with 1 μM ACh and 10 μM quinacrine. Under these conditions, rapid sealing allowed us to record channel activity in the absence and presence of quinacrine on the same patch. During the first minute, the channel activity is similar to that observed in the absence of quinacrine, with opening events typical of adult muscle nAChRs (Bouzat et al., 1994, 1998). After a few minutes, a dramatic decrease in channel activity is observed because of the diffusion of quinacrine to the tip of the pipette (Fig. 1a). The frequency of opening events decreases more than 90% at 10 μM quinacrine (Fig. 1b). The decrease in the frequency of channel opening is seen in the closed-time histogram as a displacement of the predominant closed component to longer durations (13.3 ms and 76.3 ms for t = 1 min and t = 8 min, respectively; Fig. 1c). Open-time distributions of nAChRs recorded in the presence of 10 μM quinacrine are similar to control histograms (Fig. 1c, 1.07 ms and 870 μs for t = 1 min and t = 8 min, respectively). Quinacrine does not affect the channel amplitude; the amplitudes were 5.2 ± 0.2 pA and 5.1 ± 0.2 pA for t = 0 and t = 8 min, respectively (n = 5).

Quinacrine Reduces the Duration of Clusters of Single-Channel Currents. To evaluate the influence of quinacrine on channel activation, clear clusters of events corresponding to a single channel were activated with 60 μM ACh. Each activation period (cluster) begins with the transition of a single receptor from the desensitized to the activatable state and terminates by returning to the desensitized state (Fig. 2, left). In these experiments, control and quinacrine recordings were performed on separate cell-attached patches.

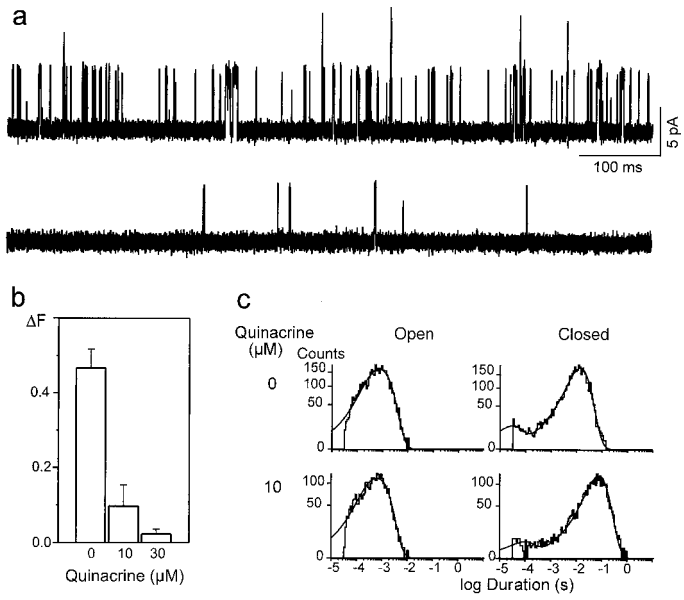

Fig. 1. Effects of quinacrine on nAChR activity. a, effects of quinacrine on the frequency of opening events. nAChR channels were recorded using a pipette containing 1 μM ACh in the tip and 1 μM ACh plus 10 μM quinacrine in the shaft. Channels were recorded immediately after seal formation (t = 1; top) and 8 min later (t = 8, bottom). Membrane potential: −70 mV. Inward currents are plotted upwards. Filter 10 kHz. b, decrease of the frequency of opening events in the presence of quinacrine. Δf is the ratio between the frequency of opening events (events per second) recorded 8 min (t = 8) and 1 min (t = 1) after seal formation. n = 4 at the specified quinacrine concentration. Data are shown as mean ± S.D. c, open- and closed-time histograms in the absence and presence of quinacrine. 0 μM, histograms corresponding to nAChR channels recorded during the first minute after rapid sealing (1 μM ACh). 10 μM, histograms corresponding to channels recorded during minute 8 after seal formation (1 μM ACh plus 10 μM quinacrine in the shaft of the pipette).

In the absence of quinacrine, closed-time histograms can be well fitted with three or four components (Fig. 2, right). Typically, there is a fast component (20–60 μs), a major intermediate component of about 0.5 to 0.8 ms that is sensitive to ACh concentration and corresponds to closings within clusters, and one or two small variable slow components associated with periods between independent activation episodes and dependent on the number of channels in the patch. In the presence of quinacrine, closed time distributions are largely affected. The relative area of the intermediate-duration component, corresponding to closings within clusters, is reduced in the presence of quinacrine (Fig. 2).

Typically, cluster duration histograms from control recordings activated by 60 μM ACh show a main component at 60 to 70 ms whose relative area is larger than 0.9 (Fig. 2). The minor component corresponds to isolated openings. As shown in Fig. 2, dramatic changes in the cluster duration histograms are observed in the presence of quinacrine. The mean cluster duration decreases to 5 and 3 ms at 10 and 30 μM quinacrine, respectively. In addition, the relative area of the brief component, corresponding to isolated events, increases with respect to that of control histograms (0.04, 0.32, and 0.33 for control, 10 μM quinacrine, and 30 μM quinacrine, respectively; Fig. 2). Open-time distributions are slightly displaced to briefer durations at 30 μM quinacrine (Fig. 2).

Dependence of Mean Cluster Duration, Openings per Cluster, Mean Open Time, and Mean Closed Time on Quinacrine Concentration. The dependence of channel kinetics on the concentration of quinacrine is shown in Fig. 3. The main effect of quinacrine is a dose-dependent reduction in the duration of clusters (Fig. 3a); this decrease is about 95% at 30 μM quinacrine. The decrease in the number of openings per cluster parallels that of cluster duration (Fig. 3b), indicating that the decrease in cluster duration is caused mainly by a decrease in the number of openings. The mean open time shows a slight concentration-dependent decrease that is statistically significant in the presence of quinacrine concentrations higher than 30 μM ($p < 0.001$) (Fig. 3c). The duration of the intermediate component of the closed-time histogram, corresponding to closings within clusters, remains stable up to 10 μM quinacrine but increases 3-fold at 60 μM (Fig. 3d). The relative area of this component decreases as a function of quinacrine concentration (Fig. 3d).

Effects of Quinacrine on nAChR as a Function of Membrane Potential. To investigate whether the action of quinacrine on the nAChR is voltage-dependent, we recorded nAChR channels activated by 60 μM ACh in the absence and presence of 10 μM quinacrine at different membrane potentials. The mean open time decreases exponentially when the membrane is depolarized for both control and quinacrine-treated channels (Fig. 4). The mean open times change e-fold per 89 and 94 mV for control and treated nAChRs, respectively. Thus the magnitude of such decrease is similar in both cases, suggesting that quinacrine does not change the intrinsic voltage dependence. The dominant effect of quinacrine is

a reduction in cluster duration. Figure 4 shows that in the presence of quinacrine, the relationship between cluster duration and membrane potential also parallels that of the control channels.

Dependence of Cluster Duration as a Function of ACh Concentration. Mean cluster duration decreases with the ACh concentration, showing values of 224 ± 10 (n = 3), 120 ± 50 (n = 3), and 60 ± 10 ms (n = 10) at 10, 30, and 60 μM ACh. The decrease in cluster duration by 10 μM quinacrine does not change with ACh concentration. This decrease is of 76 ± 7% (n = 3), 88 ± 4% (n = 3), and 85 ± 5% (n = 10) at 10, 30, and 60 μM ACh, respectively.

Effects of Quinacrine on Macroscopic nAChR Currents.

Quinacrine Increases Current Decay Due to Desensitization. To determine the overall consequences of quinacrine on nAChR activation, we studied the effect of the drug on outside-out patches rapidly perfused with 300 μM ACh. Figure 5a shows ensemble currents obtained from a single patch exposed to brief applications of ACh alone (control) and together with different concentrations of quinacrine. In control data, the current reaches the peak after 0.1 to 1 ms and then decays with a time constant (τ_d) of 44 ± 16 ms because of desensitization. When quinacrine is present in both the ACh-free and ACh-containing solutions, a concentration-dependent increase in the decay rate is observed (Fig. 5a).

At all quinacrine concentrations, decays are well fitted by a single exponential function. This was also found when currents were activated by lower concentrations of agonist (10 or 60 μM ACh, data not shown). This is in contrast to open-channel blocking drugs, which exhibit a two-component decay time course (Dilger et al., 1997; Forman, 1999), indicating that quinacrine acts mainly by increasing the rate of channel desensitization.

As shown in Fig. 5, a and b, the time constant of the decay decreases as a function of quinacrine concentration. Extrapolated peak currents obtained in the presence of 1 to 30 μM quinacrine range from 85 to 92% of control values, indicating that the drug although present in the ACh-free solution, does not affect channels when they are closed. This is in contrast to drugs that block both open and closed states of the channel.

Quinacrine Decreases the Rate of Recovery from Desensitization. The rate of recovery from desensitization was studied by using a two-pulse protocol (Dilger and Liu, 1992). After a 300-ms application of 300 μM ACh, about 90% of the channels are desensitized (Fig. 6a). The degree of recovery increases with the interval between ACh applications and more than 80% recovery is reached within 435 ms (Fig. 6a top). Recovery is dramatically slower in the continuous presence of 1 μM quinacrine (Fig. 6a, bottom).

Fig. 6b shows the relationship between the fraction of current recovery as a function of the interval duration. In the absence of quinacrine, when the time course of recovery is fit to a single exponential, the time constant (τ_r) is 168 ± 24 ms. When measurements were performed using the same protocol as in control recordings but in the presence of quinacrine, recovery is significantly delayed; τ_r is 433, 549, and 870 ms for 1, 3, and 6 μM quinacrine, respectively (Fig. 6b).

Effects of Quinacrine Application Protocol on Macroscopic Current Desensitization. In the macroscopic current experiments described thus far, patches were equilibrated with quinacrine before application of the ACh + quinacrine solution (+/+ protocol). When quinacrine is omitted from the preincubation solution (−/+ protocol), the effect of quinacrine on desensitization is less pronounced (Fig. 7). In this example, the control value of τ_d is 41.3 ms and the value of τ_d in the constant presence of 3 μM quinacrine is 4.7 ms (+/+ protocol). However, when 3 μM quinacrine is applied simultaneously with ACh, τ_d is 14.9 ms (−/+ protocol). Although quinacrine has no obvious effect on closed channels, it seems that previous incubation of the patch with quinacrine is necessary for its full action. We also looked at the effect of preincubation of the patch with quinacrine followed by application of ACh alone (+/− protocol, Fig. 7). The effect of quinacrine remains (τ_d = 6.3 ms) even though the drug is quickly removed from the aqueous solution around the patch during the +/− protocol.

In another experiment using 10 μM quinacrine, the values obtained for τ_d were: 36.8 ms (control), 5.46 ms (−/+ protocol), 2 ms (+/− protocol), and 1.59 ms (+/+ protocol), thus confirming that previous incubation of the patch with quinacrine allows a more profound increase in desensitization.

Inhibition of Embryonic-Type nAChR by Quinacrine. To determine quinacrine inhibition of embryonic nAChRs, we measured macroscopic currents activated by 300 μM ACh on BC3H-1 cells in the absence and presence of different quinacrine concentrations. As described for adult nAChRs, all current decays were fitted by a single exponential function. In the absence of quinacrine, embryonic nAChR desensitization rate is similar to that of adult nAChR (Table 1). At high quinacrine concentrations, decay time constants differ slightly from those of ϵ-containing nAChRs (Table 1). Thus, γ or ϵ subunits are not the main subunits involved in the quinacrine binding site.

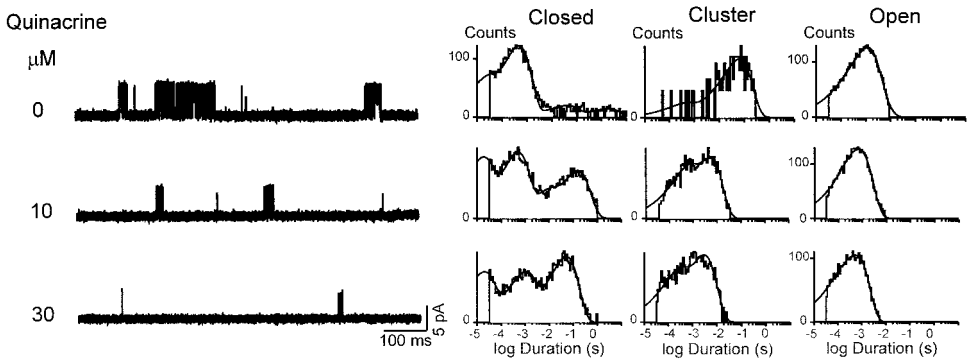

Fig. 2. Clusters of single-channel currents in the presence of quinacrine. Left, channel traces recorded in the absence and presence of 10 and 30 μM quinacrine in the pipette solution. ACh, 60 μM. Membrane potential: −70 mV. Filter, 10 kHz. Right, closed-, cluster-, and open-duration histograms corresponding to nAChRs recorded at the given quinacrine concentrations.

Effects of Quinacrine on Equilibrium Binding of ACh. To determine whether quinacrine introduces changes in equilibrium agonist binding, we compared the inhibition of α-BTX binding by ACh in the absence and presence of 10 μM quinacrine. As shown in Fig. 8, similar profiles were obtained in both cases. The apparent affinity constants (K_d) and Hill coefficients (n_H) are shown in Table 2. The calculated values for control conditions are in good agreement with those reported previously (Sine et al. 1994; Prince and Sine, 1999). Thus, although 10 μM quinacrine dramatically enhances desensitization as measured in electrophysiology experiments, no changes in the equilibrium binding of ACh are observed. Increasing quinacrine concentration from 10 to 60 μM leads to a modest shift of the curve that is statistically insignificant (Table 2). Previous work established that some noncompetitive inhibitors convert the nAChR to a state in which the affinity coincides with that of the desensitized state (Sine and Taylor, 1982). We therefore measured ACh binding in the presence of a saturating concentration of the noncompetitive inhibitor proadifen (Prince and Sine, 1998). As expected, proadifen shifts the binding curve to lower ACh concentrations and decreases the Hill coefficient to unity (Fig. 8, Table 2; Sine and Claudio, 1991; Prince and Sine, 1998). When cells are preincubated with 60 μM proadifen plus 10 μM quinacrine there is no additional shift in the binding curve (Fig. 8, Table 2).

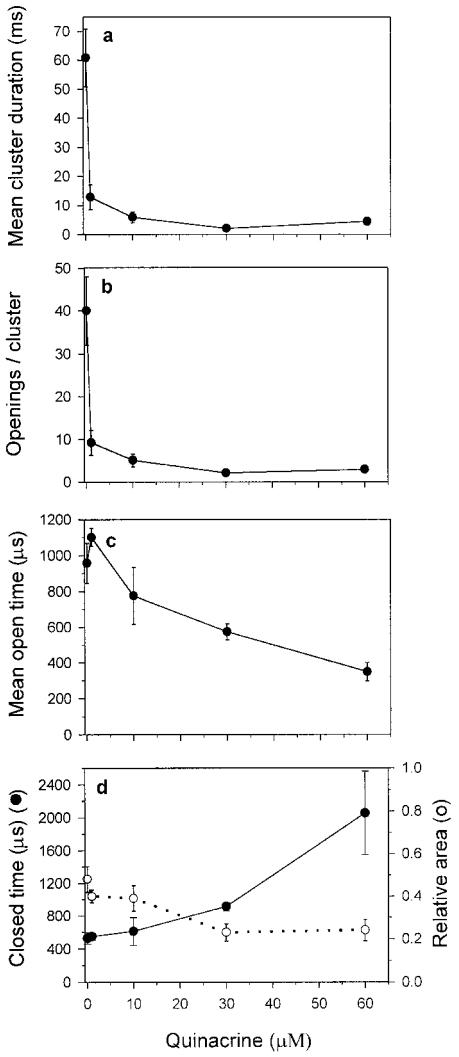

Fig. 3. Dependence of mean cluster duration (a), openings per cluster (b), mean open time (c), and mean closed time (d) on quinacrine concentration. Clusters of openings corresponding to a single channel were identified as a series of closely spaced events preceded and followed by closed intervals greater than a specified duration; this duration was taken as the point of intersection of the predominant closed time component and the succeeding one in the closed time histogram. The mean open time was obtained from the corresponding open-time histograms. The closed time and its relative area corresponds to the intermediate closed component of the closed time histogram. Data are shown as mean ± S.D. for three to eight experiments for each condition.

Discussion

Here we identify the mechanistic bases for the noncompetitive action of quinacrine: increase in the rate of desensitization together with stabilization of a desensitized state. At the single-channel level, the main effect of quinacrine is a profound decrease in the frequency of openings. Analysis of single channels activated by high concentrations of ACh permits a better understanding of the mechanistic bases of quinacrine action. Under these conditions, single-channel openings are clustered into unambiguous activation periods (Sakmann et al., 1980). A cluster starts when one nAChR recovers from desensitization and continues with the receptor undergoing cycles of agonist association/dissociation and channel gating. Auerbach and Akk (1998) demonstrated that the value of $(\tau_c P_o)^{-1}$ (where τ_c is the mean cluster duration and P_o is the probability of being open within a cluster) is a direct measure of the rate constant of desensitization. Under control conditions with 60 μM ACh, we find $P_o = 0.7$ and $\tau_c = 61 \pm 10$ ms, so that $(\tau_c P_o)^{-1} = 24 \pm 5\ s^{-1}$. This agrees with desensitization rates calculated from the decay of macroscopic currents (Dilger and Liu, 1992; Franke et al., 1993). The duration of clusters decreases in the presence of quinacrine, mainly because of a decrease in the number of successive openings. The early termination of clusters suggests that quinacrine increases the desensitization rate. Between 1 and 10 μM quinacrine, P_o is similar to control values (0.7), but there is a slight decrease at 30 μM quinacrine ($P_o = 0.55$).

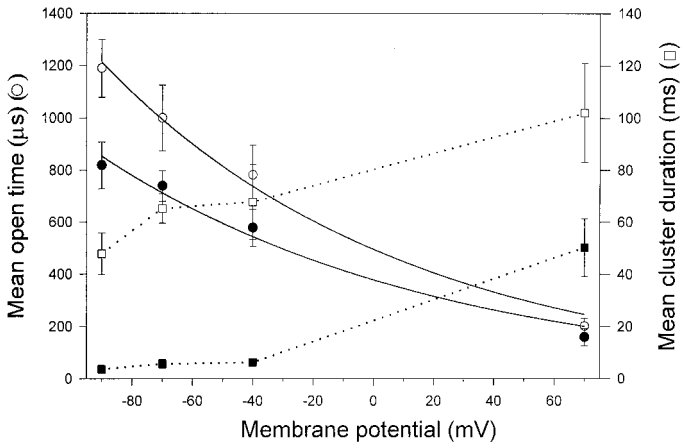

Fig. 4. Effects of quinacrine on nAChR as a function of membrane potential. nAChRs activated by 60 μM ACh were recorded in the absence (open symbols) or presence of 10 μM quinacrine (solid symbols) at different membrane potentials. Dependence of the mean open time (circles and solid line) and cluster duration (squares and dotted line) on the membrane potential. The voltage dependence of the mean open-time constant is fitted by a simple exponential decay. Data were obtained from the corresponding histograms and are expressed as the mean ± S.D. of 4 to 10 different patches.

The desensitization rate, estimated by the product $(\tau_c P_o)^{-1}$, is 122 ± 50, 280 ± 80, and 1190 ± 300 s^{-1} in the presence of 1, 10, and 30 μM quinacrine, respectively.

Conclusions obtained from single-channel recordings are in good agreement with those deduced from macroscopic currents activated by 300 μM ACh. The decay time constant (τ_d) for desensitization varied between 28 and 60 ms. At 300 μM ACh Popen > 0.9 and the fraction of current remaining after desensitization is less than 1% of the peak current. Thus, we can assume that $1/\tau_d$ equals the rate of desensitization from the double liganded open state, being its value of 26 ± 8 s^{-1}, and the reopening rate of desensitized nAChRs is very low (<0.3 s^{-1}). The desensitization rate thus calculated is in good agreement with that estimated from our single-channel data. Quinacrine increases the rate of desensitization to 110 ± 30, 220 ± 40, 370 ± 30, 560 ± 80, and 1100 ± 100 s^{-1} at concentrations of 1, 3, 6, 10, and 30 μM, respectively. Thus, information obtained from both single channel and macroscopic current recordings indicates that quinacrine profoundly increases the rate of desensitization in a concentration-dependent manner.

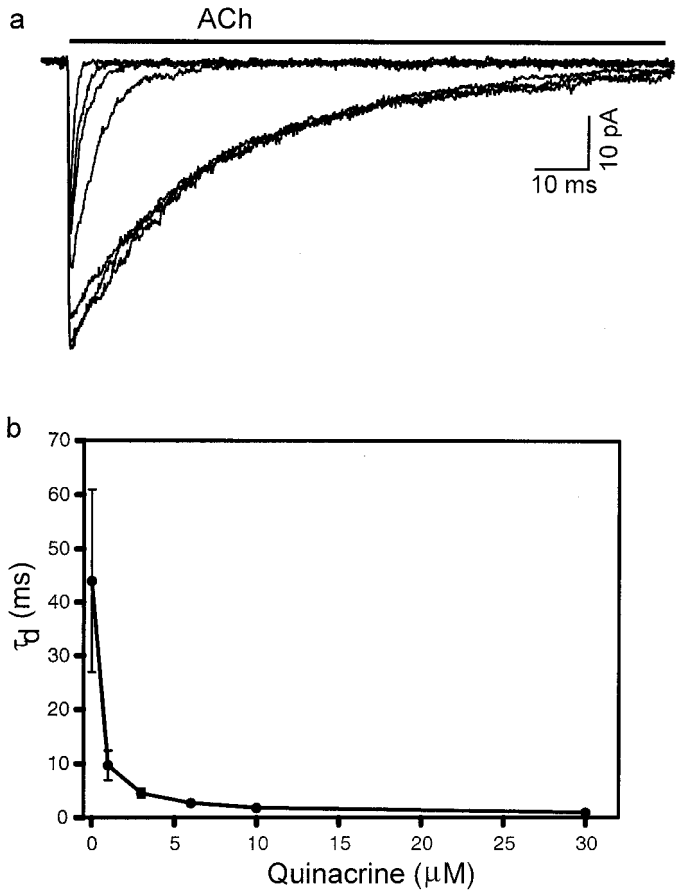

Fig. 5. Effect of quinacrine on the decay of macroscopic currents activated by 300 μM ACh. a, ensembled mean currents obtained from rapid perfusion of 300 μM ACh alone or with different concentrations of quinacrine onto an outside-out patch during 200 ms. Membrane potential of −50 mV. Each trace represents the average of 12 to 20 applications of agonist. Curves from right to the left correspond to: control (three curves), 1, 6, 10, and 30 μM quinacrine. The calculated decay time constants (τ_d) are 26.3, 26.9, and 29.1 ms for control curves and 8.3, 2.5, 1.7, and 0.86 for 1, 6, 10, and 30 μM quinacrine, respectively. b, dependence of τ_d on quinacrine concentration. Each point represents the mean ± S.D. of 3 to 13 measurements.

In the presence of quinacrine, the extrapolated peak current is similar to that of control, suggesting that quinacrine has a strong preference for interacting with the open state of the nAChR. This is consistent with the idea that quinacrine accelerates desensitization, a process that proceeds mainly from the doubly liganded open state (Dilger and Liu, 1992; Auerbach and Akk, 1998). Experiments in which quinacrine azide is used to photolabel *T. californica* nAChR also indicate that the drug binds preferentially to the open state (Johnson and Ayres, 1996).

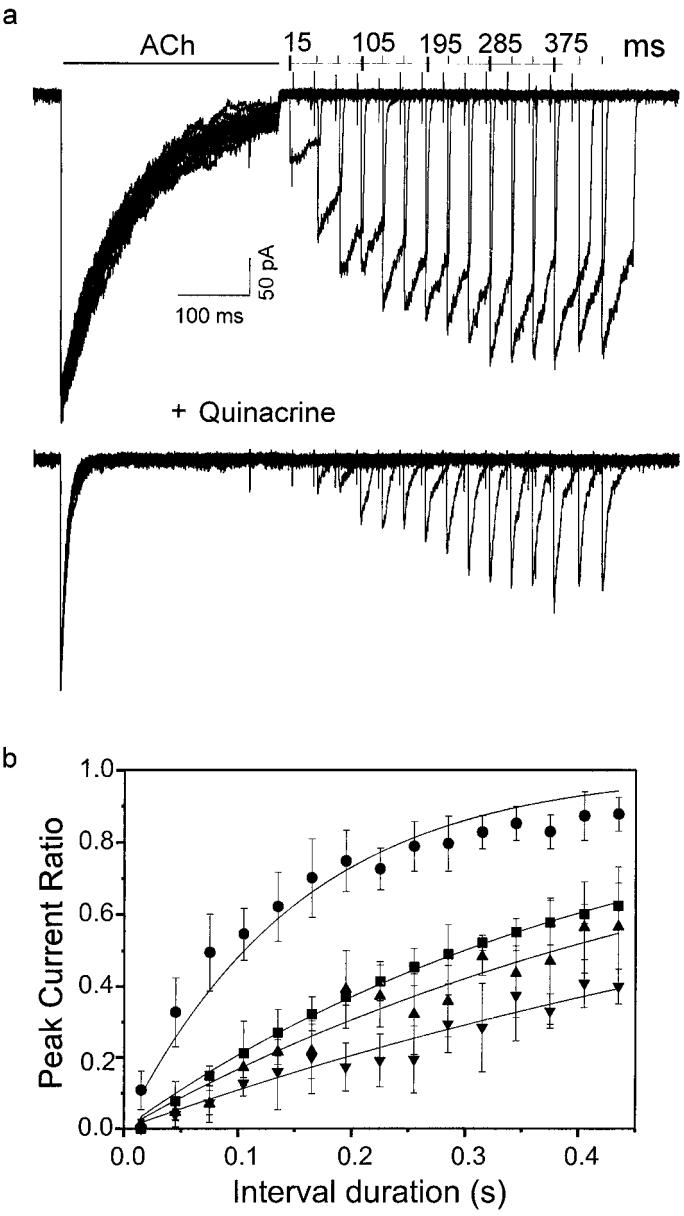

Fig. 6. Recovery from desensitization in the presence of quinacrine. a, superimposed pair of current responses to 300 μM ACh obtained using a double agonist application protocol with a variable interpulse time interval (15–435 ms). The first application lasts 300 ms and the second one is applied during 30 ms. Experiments were performed in the absence (top traces) and continuous presence of 1 μM quinacrine (bottom traces). Membrane potential, −50 mV. b, time course of recovery from desensitization. The plot show the relation of the peak current ratio with the interval between the end of the first and the beginning of the second ACh application (interval duration) for control (●), 1 (■), 3 (▲), and 6 μM (▼) quinacrine. The peak current ratio was calculated as the ratio of the peak current induced by the second pulse with respect to the first peak current.

Open channel block was the mechanism proposed for the action of quinacrine at the frog endplate nAChR (Adams and Feltz, 1980). The open channel blocking mechanism predicts that the decay should be biexponential (Dilger et al., 1997; Forman, 1999). However, we found that a single exponential function is always adequate to describe the current decay in the presence of quinacrine. This is true even for macroscopic currents activated by 60 or 10 μM ACh, for which the desensitization decay is slower. We conclude that open channel block is unlikely to be the cause of inhibition by 30 μM quinacrine. We were unable to extend the concentration range because macroscopic currents in the presence of 60 μM quinacrine were almost undetectable. Single-channel recordings in the presence of 60 μM quinacrine show a very low number of openings, but analysis of clusters suggests a slight increase in the duration of closings within clusters (Fig. 3). Because of the few openings, the duration of openings and closings within clusters at high quinacrine concentrations is less well determined than at lower concentrations. The increase in the duration of closings within clusters, together with a decrease in the mean open time could be associated with an open-channel blockade. Thus, at quinacrine concentrations higher than 30 μM, both mechanisms, increased desensitization and open channel blockade, may occur. Multiple sites of action have been described for other noncompetitive inhibitors (Spitzmaul et al., 1999). We speculate that for quinacrine, the relative occupancy of at least two sites is concentration-dependent and may also vary with the type of nAChR.

By using a two-pulse protocol, we determined the rate of recovery from desensitization in the absence of ACh, which involves agonist dissociation and return to the closed, resting state (Dilger and Liu, 1992). Recovery is slower in the presence of quinacrine, as evidenced by the 6-fold decrease in recovery rate at 6 μM quinacrine. Therefore, in addition to increase the rate of the nAChR to reach the desensitized state, quinacrine makes this state more stable.

During continued exposure to agonist, nAChR undergoes a slow conversion to a high affinity state that correlates closely with the extent of desensitization. To gain an overall mech-

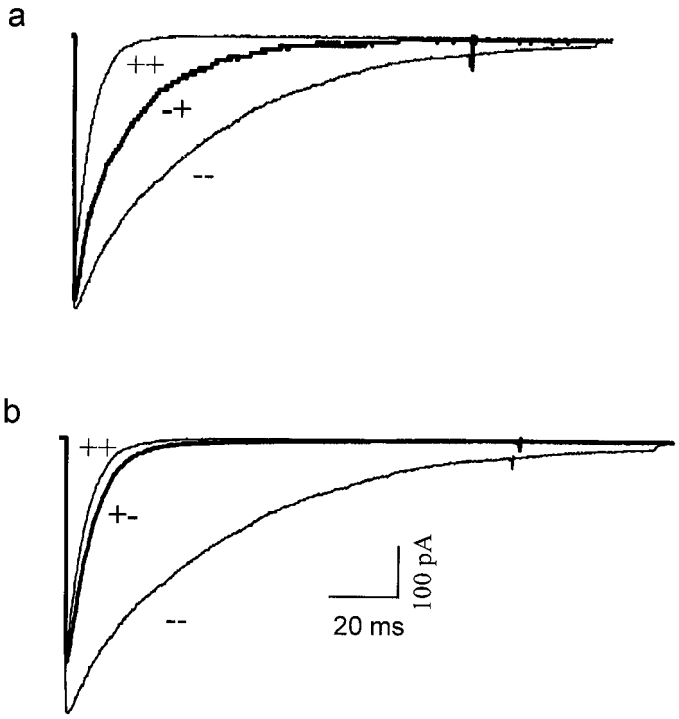

Fig. 7. Effects of quinacrine application protocol on macroscopic current desensitization. Superimposed current responses to 300 μM ACh and 3 μM quinacrine applied using different protocols. a, from right to left, curves correspond to control conditions (−/− protocol), simultaneous ACh/quinacrine application without preincubation with quinacrine (−/+ protocol), and simultaneous ACh/quinacrine application with previous incubation with quinacrine (+/+ protocol). b, from right to left, curves correspond to control conditions (−/− protocol), ACh application after the preincubation with quinacrine (+/− protocol) and simultaneous ACh/quinacrine application with previous incubation with quinacrine (+/+ protocol).

TABLE 1

Influence of quinacrine concentration and subunit composition on current decay

The table shows the decay time constants (τ_d) of currents obtained from outside-out patches exposed to 300 μM ACh containing adult ($\alpha_2\beta\varepsilon\delta$) and embryonic ($\alpha_2\beta\gamma\delta$) nAChRs. Values are expressed as the mean ± S.D. Number of experiments for each condition are shown in parentheses. Membrane potential, −50 mV.

Quinacrine	τ_d	
	$\alpha_2\beta\varepsilon\delta$	$\alpha_2\beta\gamma\delta$
μM	*ms*	
0	44.0 ± 17 (56)	41.1 ± 10.9 (31)
1	9.7 ± 2.7 (7)	12.2 ± 1.8 (5)
3	4.5 ± 0.8 (13)	6.0 ± 0.6 (3)
6	2.7 ± 0.3 (11)	3.7 ± 0.8 (5)
10	1.8 ± 0.3 (7)	2.8 ± 0.5 (3)
30	0.9 ± 0.1 (3)	

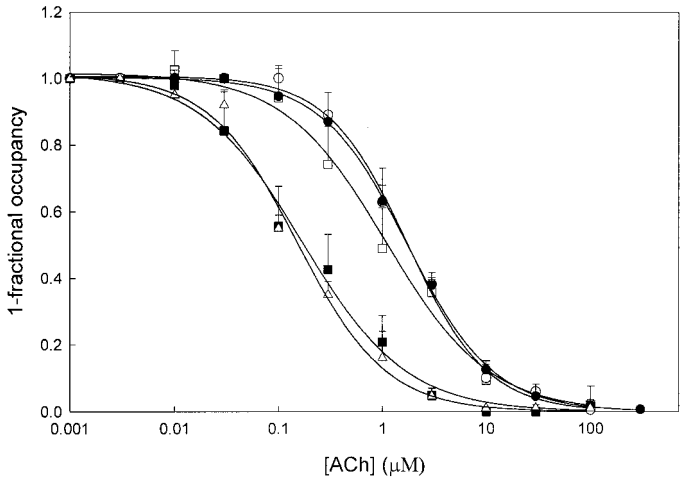

Fig. 8. Effects of quinacrine on equilibrium binding of ACh. ACh binding was measured by competition against the initial rate of α-bungarotoxin binding in the absence (○) or presence (●) of 10 μM quinacrine, 60 μM quinacrine (□), 60 μM proadifen (■), and 60 μM proadifen plus 10 μM quinacrine (△). The curves are fits to the Hill equation. Each point represents the mean ± S.D. of three to eight different experiments.

TABLE 2

Effects of quinacrine on equilibrium binding of ACh

The apparent affinity constant (K_d) and Hill coefficient (n_H) for ACh binding under the specified condition. *N* corresponds to the number of experiments.

Condition	K_d	n_H	*N*
	μM		
Control	1.90 ± 0.5	1.18 ± 0.20	7
10 μM Quinacrine	1.78 ± 0.5	1.10 ± 0.13	4
60 μM Quinacrine	1.35 ± 0.4	1.00 ± 0.21	6
60 μM Proadifen	0.14 ± 0.06	0.82 ± 0.13	8
60 μM Proadifen + 10 μM quinacrine	0.15 ± 0.06	1.00 ± 0.10	2

anistic picture of the action of quinacrine, we evaluated changes in equilibrium agonist binding. The apparent affinity of nAChRs previously equilibrated with agonist reflects a weighted average of the affinity of the agonist for the two forms of the receptor, low and high affinity, as well as the fraction of receptor in each state (Sine and Taylor, 1979). Because electrophysiological data show that quinacrine profoundly increases desensitization, we expected a shift of the curve to lower agonist concentration as observed with anesthetics (Sine and Taylor, 1982; Sine et al., 1995). Surprisingly, neither 10 μM nor 60 μM quinacrine affected the equilibrium between high and low affinity states. We also determined binding at equilibrium in the presence of proadifen. For the adult muscle nAChR, the limiting shift in affinity has been shown to occur at 30 to 60 μM proadifen (Prince and Sine, 1998). In contrast to quinacrine, 60 μM proadifen produced the expected decrease in K_d value.

An explanation for our results is that quinacrine stabilizes a conformational intermediate state of the nAChR; one that exhibits the permeability but not the agonist binding properties of desensitization. This intermediate could represent either a short-lived state that cannot be distinguished in the absence of quinacrine or a novel state induced by quinacrine.

Scheme 1 is a general model in which each state of channel activation and block is considered to have a desensitized counterpart (Dilger and Liu, 1992):

$$\begin{array}{ccccccccc} & k_1 & & k_2 & & \beta & & k_{+b} & \\ R & \leftrightarrow & AR & \leftrightarrow & A_2R & \leftrightarrow & A_2R^* & \leftrightarrow & A_2R^*A \\ & k_{-1} & & k_{-2} & & \alpha & & k_{-b} & \\ d_1 \updownarrow d_{+1} & & d_{-2} \updownarrow d_{+2} & & d_{-3} \updownarrow d_{+3} & & d_{-4} \updownarrow d_{+4} & & d_{-5} \updownarrow d_{+5} \\ & k_d^{+1} & & k_d^{+2} & & \beta^d & & k_d^{+b} & \\ D & \leftrightarrow & AD & \leftrightarrow & A_2D & \leftrightarrow & A_2D^* & \leftrightarrow & A_2D^*A \\ & k_d^{-1} & & k_d^{-2} & & \alpha^d & & k_d^{-b} & \end{array}$$

Scheme 1.

Our results from single channel-data suggest that d_{+4} in Scheme 1 is one of the main kinetic steps affected by quinacrine. However, equilibrium binding studies suggest that quinacrine stabilizes an intermediate conformation of the transition from resting to desensitized states. This conformational intermediate (A_2I) could be either in the A_2R^* to A_2D^* path or in a branched path in which both A_2I and A_2D are connected to A_2R^*.

In accordance with our results, conformational intermediates between the resting and desensitized states of the nAChR have recently been described. Ryan et al. (2001), with the use of infrared difference spectroscopy, showed that domains of the nAChR interconvert between the resting and desensitized states independently of each other and that binding to the noncompetitor inhibitor binding site may lead to the formation of a conformation that is structural intermediate between both states. Further studies using more specific techniques (Ryan et al., 2001) will be required to confirm our explanation for quinacrine's action.

Changes in the solution application protocol show that the effect of quinacrine develops and recovers slowly (i.e., between 50 ms and 5 s). One interpretation is that quinacrine binds to the nAChR closed state and dissociates slowly from this state but does not exert its effect until the channel opens. Early work from Grunhagen and Changeux (1976) used quinacrine to monitor structural changes that take place upon binding of cholinergic ligands. Interestingly, a slow equilibration process of quinacrine-treated membranes after addition of carbamylcholine was observed. The kinetics of the slow phase were interpreted to represent the time course of transitions in the nAChR, which in turn affect the energy transfer to quinacrine. Alternatively, quinacrine, because of its hydrophobicity, may require >10 ms to equilibrate with the patch membrane. In this scenario, quinacrine would have access from the membrane to its inhibitory binding site on the nAChR. Similar explanations have been proposed for the slow kinetics of action of 3-(trifluoromethyl)-3-(*m*-iodophenyl)diazirine (Forman, 1999).

Arginine209 and Proline211 of the αM1 transmembrane domain have been specifically photolabeled by quinacrine azide (Cox et al., 1985; DiPaola et al., 1990). The disposition and functional role of the M1 transmembrane domain remain uncertain. Our results reveal that M1 may contribute to the desensitization process.

Acknowledgments

We thank Dr. S. Sine and Nina Bren for advice on ligand binding measurements.

References

Adams PR and Feltz A (1980) Quinacrine (mepacrine) action at frog end-plate. *J Physiol* **306:**261–281.
Akabas M and Karlin A (1995) Identification of acetylcholine receptor channel-lining residues in the M1 segment of the α-subunit. *Biochemistry* **34:**12496–12500.
Arias HR (1997) The high-affinity quinacrine binding site is located at a non-annular lipid domain of the nicotinic acetylcholine receptor. *Biochim Biophys Acta* **1347:** 9–22.
Arias HR (1998) Binding sites for exogenous and endogenous non-competitive inhibitors of the nicotinic acetylcholine receptor. *Biochim Biophys Acta* **1376:**173–220.
Arias HR, Valenzuela CF and Johnson DA (1993) Quinacrine and ethidium bind to different loci on the Torpedo acetylcholine receptor. *Biochemistry* **32:**6237–6242.
Auerbach A and Akk G (1998) Desensitization of mouse Nicotinic Acetylcholine Receptor channels. A two-gate mechanism. *J Gen Physiol* **112:**181–197
Bouzat C, Bren N and Sine SM (1994) Structural basis of the different gating kinetics of fetal and adult nicotinic acetylcholine receptors. *Neuron* **13:**1395–1402.
Bouzat C, Roccamo AM, Garbus I and Barrantes FJ (1998) Mutations at lipid-exposed residues of the acetylcholine receptor affect its gating kinetics. *Mol Pharmacol* **54:**146–153.
Blanton MP and Cohen JB (1994) Identifying the lipid-protein interface of the *Torpedo* nicotinic acetylcholine receptor: secondary structure implications. *Biochemistry* **33:**2859–2872.
Cox RN, Kaldany RR, DiPaola M and Karlin A (1985) Time-resolved photolabeling by quinacrine azide of a noncompetitive inhibitor site of the nicotinic acetylcholine receptor in a transient, agonist-induced state. *J Biol Chem* **260:**7186–7193.
Dilger JP, Boguslavsky R, Barann M, Katz T and Vidal AM (1997) Mechanisms of barbiturate inhibition of acetylcholine receptor channels. *J Gen Physiol* **109:**401–414.
Dilger JP and Liu Y (1992) Desensitization of acetylcholine receptors in BC3H-1 cells. *Pfluegers Arch* **420:**479–485.
DiPaola M, Kao PN and Karlin A (1990) Mapping the α-subunit site photolabeled by the noncompetitive inhibitor [^{3}H]quinacrine azide in the active state of the nicotinic acetylcholine receptor. *J Biol Chem* **265:**11017–11029.
Forman SA (1999) A hydrophobic photolabel inhibits Nicotinic Acetylcholine Receptors via open-channel block following a slow step. *Biochemistry* **38:**14559–14564.
Franke P, Parnas H, Hovav G and Dudel J (1993) A molecular scheme for the reaction between acetylcholine and nicotinic channels. *Biophys J* **64:**339–356.
Fu D-X and Sine SM (1996) Asymmetric contribution of the conserved disulfide loop to subunit oligomerization and assembly of the nicotinic acetylcholine receptor. *J Biol Chem* **271:**31479–31484.
Grunhagen H-H and Changeux J-P (1976) Studies on the electrogenic action of acetylcholine with *Torpedo marmorata* electric organ. *J Mol Biol* **106:**517–535.
Hamill OP, Marty A, Neher E, Sakmann B and Sigworth FJ (1981) Improved patch-clamp techniques for high-resolution current recording from cells and cell-free membrane patches. *Pfluegers Arch* **391:**85–100.
Johnson DA and Ayres S (1996) Quinacrine noncompetitive inhibitor binding site localized on the *Torpedo* acetylcholine receptor in the open state. *Biochemistry* **35:**6330–6336.
Liu Y and Dilger JP (1991) Opening rate of acetylcholine receptor channels. *Biophys J* **60:**424–432.
Prince RJ and Sine SM (1998) Epibatidine binds with unique site and state selectivity to muscle nicotinic acetylcholine receptors. *J Biol Chem* **273:**7843–7849.
Prince RJ and Sine SM (1999) Acetylcholine and epibatidine binding to muscle acetylcholine receptors distinguish between concerted and uncoupled models. *J Biol Chem* **274:**19623–19629.

Ryan SE, Blanton MP and Baenziger JE (2001) A conformational intermediate between the resting and desensitized states of the nicotinic acetylcholine receptor. *J Biol Chem* **276:**4796–4803.
Sakmann BJ, Patlak J and Neher E (1980) Single acetylcholine-activated channels show burst-kinetics in the presence of desensitizing concentrations of agonist. *Nature (Lond)* **286:**71–73.
Sine SM and Claudio T (1991) γ- and δ-subunits regulate the affinity and the cooperativity of ligand-binding to the acetylcholine receptor. *J Biol Chem* **266:** 19369–19377.
Sine SM, Kreienkamp HJ, Bren N, Maeda R and Taylor P (1995) Molecular dissection of subunit interfaces in the acetylcholine receptor: identification of determinants of alpha-conotoxin M1 selectivity. *Neuron* **15:**205–211.
Sine SM, Quiram P, Papanikolaou F, Kreienkamp HJ and Taylor P (1994) Conserved tyrosines in the alpha subunit of the nicotinic acetylcholine receptor stabilize quaternary ammonium groups of agonists and curariform antagonists. *J Biol Chem* **269:**8808–8816.
Sine SM and Taylor P (1979) Functional consequences of agonist-mediated state transitions in the cholinergic receptor. *J Biol Chem* **254:**3315–3325.
Sine SM and Taylor P (1982) Local anesthetics and histrionicotoxin are allosteric inhibitors of the acetylcholine receptor. *J Biol Chem* **257:**8106–8114.
Spitzmaul GF, Esandi MC and Bouzat C (1999) Amphetamine acts as a channel blocker of the acetylcholine receptor. *Neuroreport* **10:**2175–2181.
Tamamizu S, Todd AP and McNamee MG (1995) Mutations in the M1 region of the icotinic acetylcholine receptor alter the sensitivity to inhibition by quinacrine. *Cell Mol Neurobiol* 15: 427–438.
Valenzuela CF, Kerr JA and Johnson DA (1992) Quinacrine binds to the lipid-protein interface of the *Torpedo* acetylcholine receptor: a fluorescence study. *J Biol Chem* **267:**8238–8244.

Address correspondence to: Dr. Cecilia Bouzat, Instituto de Investigaciones Bioquímicas, UNS-CONICET. Camino La Carrindanga Km 7- 8000 Bahía Blanca-Argentina. E-mail: inbouzat@criba.edu.ar